Available online at www.sciencedirect.com
ScienceDirect
Polymer 48 (2007) 7414–7418
polymer
www.elsevier.com/locate/polymer

Studies on fluorinated polyurethanes by X-ray diffraction and density functional theory calculations with periodic boundary conditions

Li-Fen Wang*

Department of Applied Chemistry, Fooyin University, 151 Chin-Hsueh Road, Ta-Liao Hsiang, Kaohsiung 831, Taiwan, ROC

Received 8 August 2007; received in revised form 8 October 2007; accepted 8 October 2007
Available online 22 October 2007

Abstract

Thin-film wide-angle X-ray diffraction, small-angle X-ray scattering, and density functional theory calculations using B3LYP hybrid functional with the two-dimensional periodic boundary conditions (2D-PBC) have been applied to study the crystal structures of parent and fluorinated polyurethanes. The crystal structures from 2D-PBC-B3LYP calculation and experiments showed the hard-segment chains within crystallites adopted an extended-chain conformation for polyurethanes. Energetically, the parent polyurethane preferred an alternating hydrogen-bonded sheet structure while the fluorinated one adopted a progressive hydrogen-bonded sheet structure.
© 2007 Published by Elsevier Ltd.

Keywords: Fluorinated polyurethane; Density functional calculations; Periodic boundary conditions

1. Introduction

Fluorinated polyurethanes (FPUs) had excellent thermal and oxidative stability, low surface tension, low friction, good chemical resistance, and good compatibility with blood in biomedical applications [1–6]. Also, incorporation of fluorine into polyurethanes (PUs) altered the morphology of PUs and had an effect on their biocompatibility [7–11]. Thus it is important to elucidate the fluorination effects on the structure and conformational properties of parent PU.

Previous investigation [12] used the 1,4-di-(3′-propylcarbamate)butane and 2,2,3,3-tetrafluoro-1,4-di-(3′-propylcarbamate)-butane, designated as U and T, respectively, as monomeric compounds to model urethane units in 1,4-butanediol and 2,2,3,3-tetrafluoro-1,4-butanediol chain-extended polyurethanes, respectively. The monomeric compound consisted of a repeat unit of hard segment. A density functional theory (DFT) calculation with Becke's three-parameter hybrid functional [13] using the correlation functional (containing both local and nonlocal terms) of Lee, Yang and Parr (LYP) [14] (B3LYP) and the 6-31G(d′, p′) basis set that originated from the 6-31G† and 6-31G†† basis sets of Petersson and coworkers [15,16] gave quantitative understandings on hydrogen bonds and demonstrated experimental results of differential scanning calorimetry and infrared spectra. To further elucidate the effect of fluorination on the crystal structure of the parent PU, thin-film wide-angle X-ray diffraction (WAXD), small-angle X-ray scattering (SAXS) and first principle B3LYP calculation with two-dimensional periodic boundary conditions [17–19] (2D-PBC) were used to investigate the parent and fluorinated polyurethanes in this study.

2. Methods

2.1. Materials

The fluorinated (FB-sample) and parent (BD-sample) polyurethanes were synthesized using hexamethylene diisocyanate (HDI; Aldrich), poly(tetramethyl oxide) (PTMO, 650 g/mol; Aldrich), and chain extender (2,2,3,3-tetrafluoro-1,4-butanediol

* Tel.: +886 7 7811151x613; fax: +886 7 7826732.
E-mail address: sc112@mail.fy.edu.tw

0032-3861/$ - see front matter © 2007 Published by Elsevier Ltd.
doi:10.1016/j.polymer.2007.10.017

(FB; Lancaster) and 1,4-butanediol (BD; Tedia) for FB-sample and BD-sample, respectively) in 2:1:1, 3:1:2 and 4:1:3 stoichiometry [12]. The chemical compositions of studied polyurethanes, FB-*nlm* and BD-*nlm*, of which the soft segments were uniform in length, are listed in Table 1. In this notation, the list of three numbers, *nlm*, was the stoichiometric molar ratio of HDI:PTMO:chain extender.

2.2. X-ray diffraction

SAXS experiments were performed using Cu Kα radiation of wavelength 1.542 Å from a Rigaku rotating anode operating at 45 kV and 0.67 mA (Osmic, USA; PSAXS-USH-WAXS-002). Beam spot size of 30 × 30 μm was used, and segmented beam allowed the detector to move closer to the sample for measuring *d*-spacings smaller than 0.2 nm. The detector was placed in an off-center position in order to cover a broad range of scattering vectors, $k = (4\pi/\lambda)\sin(2\theta)$, with λ the wavelength and 2θ the scattering angle, ranging from 0.054 nm^{-1} to 1.6 nm^{-1}. Thin-film WAXD studies were recorded using a Rigaku X-ray diffractometer (D/MAX 2500) with 18 kW Cu Kα radiation ($\lambda = 1.542$ Å).

Table 1
Material compositions and domain thickness from SAXS results and 2D-PBC-B3LYP calculations

Polyurethane[a]	Hard-segment composition	SAXS		2D-PBC-B3LYP
		L	D_h	$D_{h,calc}$
BD-211	HDI–BD–HDI	82.9	28.6	20.6
BD-312	$(HDI–BD)_2$–HDI	97.1	39.1	33.2
BD-413	$(HDI–BD)_3$–HDI	114.3	56.1	45.8
FB-211	HDI–FB–HDI	85.7	31.4	23.5
FB-312	$(HDI–FB)_2$–HDI	100.0	41.5	37.3
FB-413	$(HDI–FB)_3$–HDI	122.9	59.2	51.3

All dimensions are listed in Å.
[a] All polyurethanes were synthesized using PTMO (650 g/mol) as the soft segment.

2.3. Quantum chemical calculations

All calculations were carried out by means of Gaussian 03 program [20]. A unit cell containing one and two repeating units of hard-segment with all-*trans* configuration has been adopted to construct the starting structures of progressive and alternating models, respectively (Fig. 1).

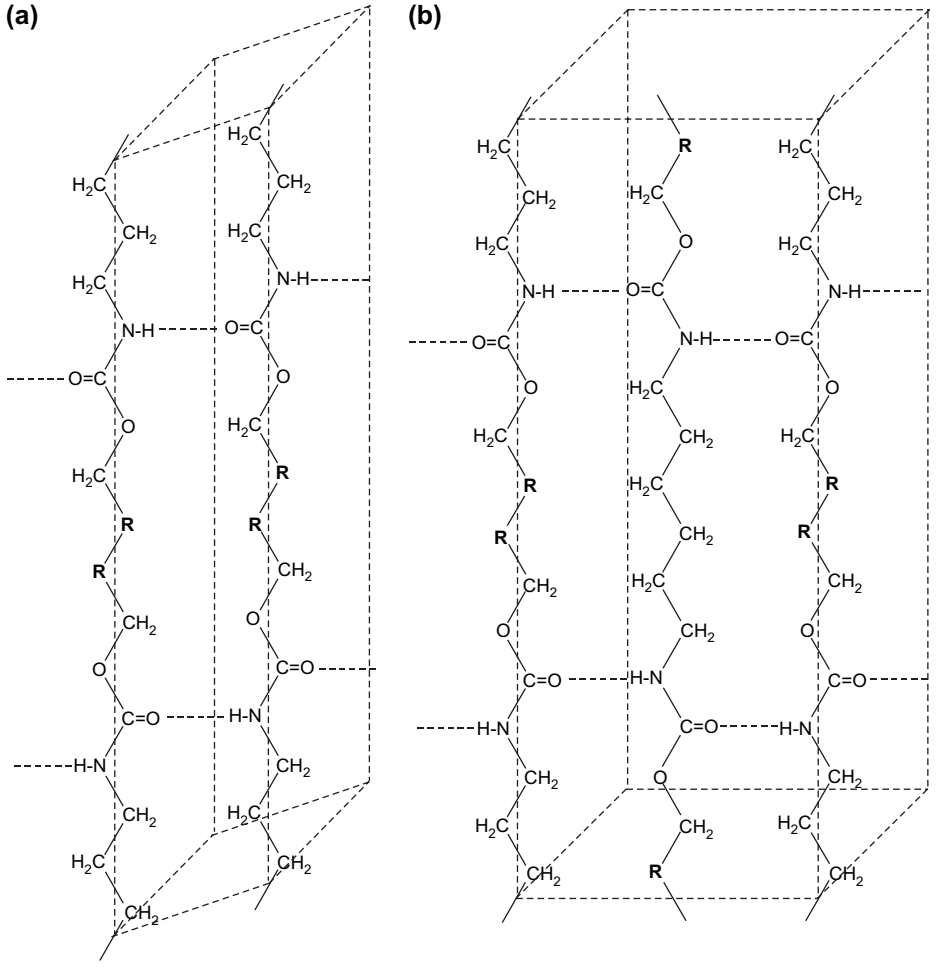

Fig. 1. Schematic unit cell structures of polyurethanes: (a) progressive and (b) alternating chain shear models. Group R denotes $-CF_2-$ and $-CH_2-$ for FB and BD-samples, respectively. The hydrogen bonding in these complexes is indicated by a dotted line.

The interaction energies of molecular complexes of U–U and T–T were calculated by B3LYP with various combinations of basis sets to measure the performance of different basis sets. Calculated results are shown in Table 2. It was noted that a simplified scheme in which consisting of the 3-21G* basis set for the carbon, the 6-31G(d, p) basis set for the hydrogen and the basis set of 6-31G(d′) for the oxygen, nitrogen, and fluorine gave calculated values consistent with the B3LYP/6-31(d′,p′) calculated results (with energy differences less than 0.2%). Therefore we adopted the simplified combination of basis sets carry out all 2D-PBC-B3LYP calculations to reduce computational cost.

3. Results and discussion

3.1. Experimental

Fig. 2 displayed the one-dimensional (γ_1) and three-dimensional (γ_3) correlation functions of the FB-413 from SAXS measurements. The non-exponential decay in three-dimensional correlation function and the exhibited periodicity in one-dimensional correlation function indicated an existence of two-phase structure, which can be described as alternating layers of hard- and soft-segment domains [11,21]. All samples showed a similar feature in the SAXS measurement. Table 1 lists the estimates of the hard-segment domain thickness, D_h and $D_{h,calc}$, and the inter-domain spacing, $L = D_h + D_s$, based on the positions of the primary minimum and the maximum in one-dimensional correlation function from SAXS [22,23] (Fig. 2) and 2D-PBC-B3LYP calculations. The D_s is the soft-segment domain thickness. It was found that both hard-segment domain thickness (D_h) and inter-domain spacing (L) increase significantly with lengthening hard-segment. This suggested that the hard-segment chains are in an extended-chain conformation [23,24].

Fig. 3 shows the WAXD results for BD- and FB-sample (the WAXD pattern of FB-312 has been shown in previous paper [25]). The observed diffraction positions exhibited a remarkable dependence on the type of hard-segment (chain extender BD or FB), but not the hard-segment length. All the BD-samples appeared two strong diffraction peaks at $d = 4.4$ Å and 3.7 Å ($2\theta = 20°$ and 24°, respectively) and a weak diffraction peak at spacing $d = 6.3$ Å ($2\theta = 14°$) (Table 3). The two peaks at $d = 4.4$ Å and 3.7 Å are similar to the strong diffraction at a d-spacing of 4.5–4.7 Å and 3.7–3.8 Å in other aliphatic m, n-polyurethanes [O–$(CH_2)_m$–O–C(O)NH–$(CH_2)_n$–NHC(O)–]$_x$ ($m = 12$, 22, 32 and $n = 4$, 6,

Table 2
Interaction energies[a] (kJ/mol) of the complexes in monomeric systems by using B3LYP method with different basis sets

Basis set	U–U	T–T
All atoms: 6-31G(d′, p′)[b]	60.4	54.6
C: 3-21G*; H, O, N, F: 6-31G(d′, p′)	61.4	55.5
C: 3-21G*; H: 6-31G(d′, p′); O, N, F: 6-31G(d′)	61.4	55.5
C: 3-21G*; H: 6-31G(d, p); O, N, F: 6-31G(d′)	61.6	55.7

[a] The energy differences between the sum energy of both individual molecules and the complex energy.
[b] Calculated results from the previous study [12].

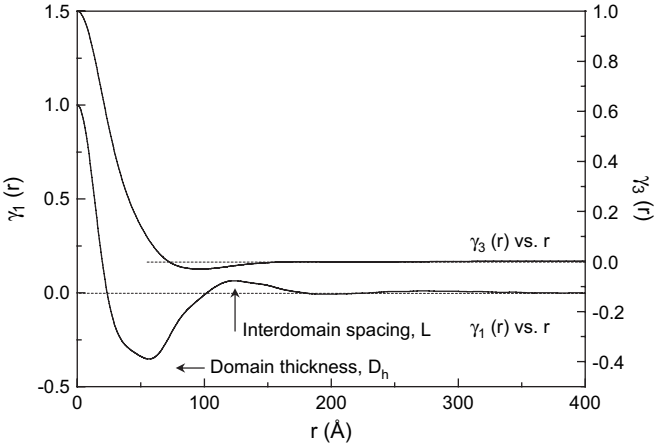

Fig. 2. One-dimensional (γ_1) and three-dimensional (γ_3) correlation functions of FB-413 sample.

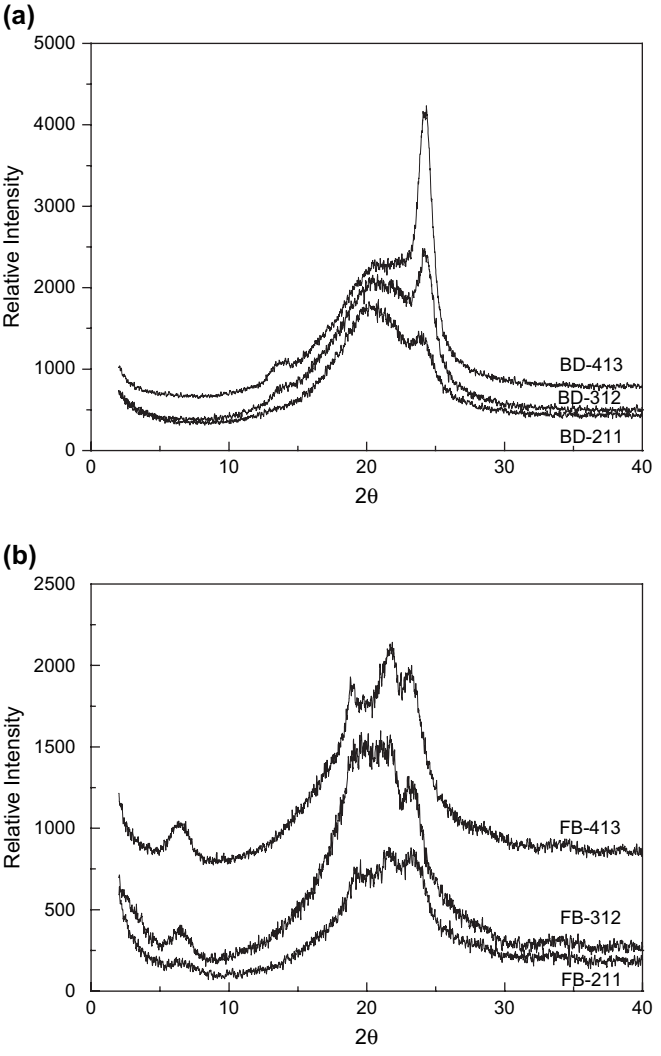

Fig. 3. Thin-film WAXD patterns of (a) BD-samples and (b) FB-samples. The curves have been shifted vertically for clarity.

Table 3
Comparison of observed *d*-spacings (WAXD) and calculated unit cell parameters

BD-sample				FB-sample			
WAXD		2D-PBC-B3LYP		WAXD		2D-PBC-B3LYP	
(200)	4.4	*a*	9.6	(100)	4.7	*a*	4.9
(010)	3.7	*b*	–	(200)[a]	4.2		
(002)	6.3	*c*	19.4	(010)	3.9	*b*	–
				(001)	14.0	*c*	16.3
		β	90.0			*β*	80.9

Distances in Å and angles in degrees.
[a] The diffraction spacing is identified with the presence of some pseudohexagonal crystal structure [27,29].

8, 12, respectively) [26]. In this study, BD-samples have $m = 4$ and $n = 6$, respectively. Several studies [26–29] have shown that aliphatic polyurethanes have a similar crystal structure as their corresponding nylons. These two strong diffraction peaks appear to be related to the characteristic 4.4 Å (indexed as 100 diffraction signal) and 3.7 Å (010 diffraction signal) for even–even nylons, $[NH-(CH_2)_m-NH-C(O)-(CH_2)_n-C(O)-]_x$, and even nylons, $(-NH-(CH_2)_m-C(O)-)_x$. Accordingly, the *d*-spacings of 4.4 Å and 3.7 Å in BD-samples represent a projected interchain distance within a hydrogen-bonded sheet and the intersheet distance, respectively. A weaker peak appearing at 6.3 Å came from the reflection of structure repeat (*c*-axis), depending on the hard-segment structure and tilt angle [30,31]. FB-samples exhibited three interchain reflections at 4.7, 4.2, and 3.9 Å ($2\theta = 18.8°$, 21.2° and 23.1°, respectively). The *d*-spacing of 14.0 Å ($2\theta = 6.3°$) presenting the *c*-axis of crystallite was noted to be doubled the spacing of 6.3 Å for BD-samples.

3.2. Quantum chemical calculations

Figs. 4 and 5 show the 2D-PBC-B3LYP optimized structures for BD- and FB-sample, respectively. For BD-samples, the chains appeared in planar zigzag structures with two possible hydrogen-bonded sheets (*ac* plane), progressive or alternating chain shear model [31–34]. Fig. 4(a) show the progressive structure in which the chains progressively sheared by 12.2° parallel to the chain axis (*c*-axis) and all the urethane units created linear –C═O···H–N– hydrogen bonds to maximize the overall stability of the crystal structure. This hydrogen-bonding pattern is commonly found in even–even nylons, for instance, nylon 6,6 [32–35]. Fig. 4(b) showed the alternating shear chains in which the arrangement between adjacent chains is alternating up and down. This was typically observed in even nylons (e.g., nylon 6) [36,37].

The changes in energy relative to the corresponding one-dimensional PBC-B3LYP calculated values for progressive and alternating models of BD-sample were 61.5 kJ/mol and 66.0 kJ/mol, respectively. This suggested that BD-sample preferred to adopt the alternating arrangement, resulting in only the 002 diffraction signal appeared in WAXD patterns while the 001 diffraction signal was absent [30,31]. Accordingly, a *d*-spacing projected from half of hard-segment repeat will

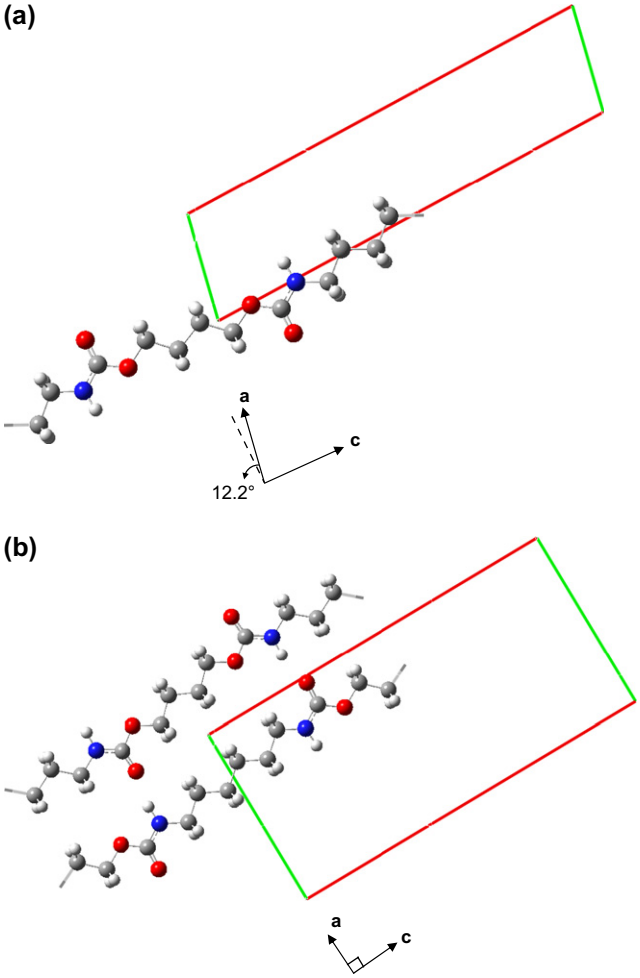

Fig. 4. 2D-PBC-B3LYP optimized structures for BD-samples: (a) progressive and (b) alternating chain shear models. Key: red, oxygen; blue, nitrogen; black, carbon; white, hydrogen. (For interpretation of the references to colour in this figure legend, the reader is referred to the web version of this article.)

be generated. Compared with the experimental observation, the WAXD-based *d*-spacing of 6.3 Å is less than half of the estimated hard-segment repeat (19.4 Å), thus the prediction from 2D-PBC-B3LYP calculations is consistent with the WAXD results.

The FB-samples preferred to adopt a progressive chain shear structure (Fig. 5) because distorted chains occurring in the local region of the coupled ester–amide backbone destroy the hydrogen bond network in alternating model. The calculated dihedral angle of $-CF_2-CH_2-O-C(O)-$ was 116°, distorted 64° from all-*trans* conformation having an angle of $-CF_2-CH_2-O-C(O)-$ in 180°. The distortion was mainly attributed to the steric hindrance of bulkier fluorine than hydrogen [12]. In good agreement with the WAXD measurement, the estimated hard-segment repeat (16.3 Å) was close to the appeared *d*-spacing of 14.0 Å. Based on an analog with nylon 6,6, the diffraction spacings of 4.7 Å and 3.9 Å denote the interchain (*a*-axis) and the intersheet (*b*-axis) distances, whereas 4.2 Å is often identified with the presence of some pseudohexagonal crystal structure [26,27].

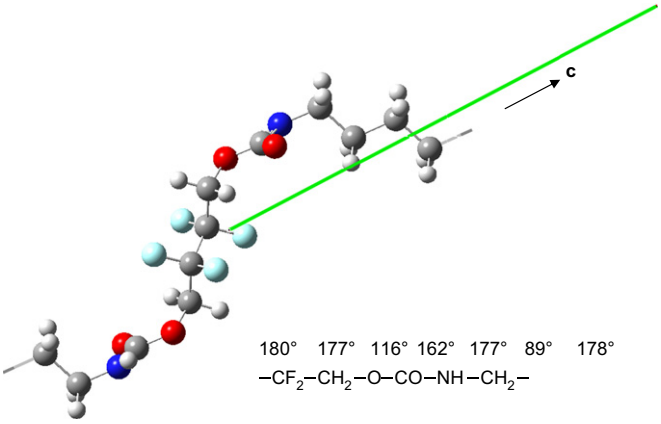

Fig. 5. 2D-PBC-B3LYP optimized structures for FB-samples (view parallel to the *a*-axis). Key: red, oxygen; blue, nitrogen; black, carbon; white, hydrogen; green, fluorine. (For interpretation of the references to colour in this figure legend, the reader is referred to the web version of this article.)

Based on the optimized structures of BD- and FB-sample, the calculated a, c and β–angle parameters are also listed in Table 3 with the WAXD-determined values. The ratio of the measured spacing of the 001 signal and the calculated c-axis value gave estimates of the angle of chain tilt with respect to the lamellar surface normal, i.e., $\cos^{-1}$ (2 × 6.3 Å/19.4 Å) = 49.5° for BD-sample and $\cos^{-1}$ (14.0 Å/16.3 Å) = 30.8° for FB-sample [26,31]. According to the optimized geometries of BD- and FB-sample, the estimated domain thickness ($D_{h,calc}$) as listed in Table 1 corresponded very well to the SAXS results. That is, the morphologies of both the samples consist of long stacks of associated hard-segments embedded in the soft-segment phase. Because the SAXS scattering intensity arises due to local heterogeneities in the electron density of sample, the differences between measured and calculated hard-segment domain thickness should attribute to the existence of phase-mixing region between the hard and soft phases [11,22–24].

4. Summary

In agreement with the experimental observations of SAXS and WAXD measurements, 2D-PBC-B3LYP calculations provided an understanding on the crystal structures of the parent and fluorinated polyurethanes. The BD- and FB-sample adopted alternating and progressive hydrogen-bonded sheet structure, respectively. The calculated geometries showed that the hard-segment chains in the crystallites of BD-samples were in planar zigzag structures while FB-samples had a local rotation at the termini of the ester–amide coupled units. This was attributed to the steric hindrance of fluorine. The distorted chains made the alternating hydrogen-bonded sheet structure unstable. Calculated values in hard-segment domain thickness of BD- and FB-sample with SAXS measurements illustrated that the hard-segment chains within crystallites adopted extended-chain conformation.

Acknowledgements

The author thanks the National Science Council, Taiwan, Republic of China, for financially supporting this research under Contract No. NSC 95-2221-E-242-008. We are also grateful to the National Center for High-performance Computing (NCHC) for computer time and facilities.

References

[1] Yu XH, Okkema AZ, Cooper SL. J Appl Polym Sci 1990;41:1777.
[2] Massa TM, Yang ML, Ho JYC, Brash JL, Santerre JP. Biomaterials 2005;26:7367.
[3] Tan H, Guo M, Du R, Xie X, Li J, Zhong Y, et al. Polymer 2004;45:1647.
[4] Tan H, Li J, Guo M, Du R, Xie X, Zhong Y, et al. Polymer 2005;46:7230.
[5] Kim YS, Lee JS, Ji Q, McGrath JE. Polymer 2002;43:7161.
[6] McCloskey CB, Yip CM, Santerre JP. Macromolecules 2002;35:924.
[7] Tonelli C, Ajroldi G, Turturro A, Marigo A. Polymer 2001;42:5589.
[8] Grasel TG, Cooper SL. Biomaterials 1986;7:315.
[9] Hsu SH, Lin ZC. Colloids Surf B Biointerf 2004;36:1.
[10] Huang SL, Chao MS, Ruaan RC, Lai JY. Eur Polym J 2000;36:285.
[11] Tonelli C, Ajroldi G, Marigo A, Marego C, Turturro A. Polymer 2001;42:9705.
[12] Wang LF. Polymer 2007;48:894.
[13] Becke AD. J Chem Phys 1993;98:5648.
[14] Lee C, Yang W, Parr RG. Phys Rev B 1988;37:785.
[15] Petersson GA, Al-Laham MA. J Chem Phys 1991;94:6081.
[16] Petersson GA, Bennett A, Tensfeldt TG, Al-Laham MA, Shirley WA, Mantzaris J. J Chem Phys 1988;89:2193.
[17] Improta R, Barone V, Kudin KN, Scuseria GE. J Chem Phys 2001;114:2541.
[18] D'Amore M, Talarico G, Barone V. J Am Chem Soc 2006;128:1099.
[19] Improta R, Barone V, Kudin KN, Scuseria GE. J Am Chem Soc 2001;123:3311.
[20] Frisch MJ, Trucks GW, Schlegel HB, Scuseria GE, Robb MA, Cheeseman JR, et al. Gaussian 03, revision C.02. Wallingford, CT: Gaussian, Inc; 2004.
[21] Laity PR, Taylor JE, Wong SS, Khunkamchoo P, Norris K, Cable M, et al. Polymer 2004;45:7273.
[22] Chang SL, Yu TL, Huang CC, Chen WC, Linliu K, Li TL. Polymer 1998;39:3479.
[23] Versteegen RM, Kleppinger R, Sijbesma RP, Meijer EW. Macromolecules 2006;39:772.
[24] Li Y, Ren Z, Zhao M, Yang H, Chu B. Macromolecules 1993;26:612.
[25] Wang LF, Wei YH. Colloids Surf B Biointerf 2005;41:249.
[26] Mckiernan RL, Heintz AM, Hsu SL, Atkins EDT, Penelle J, Gido SP. Macromolecules 2002;35:6970.
[27] Genovese A, Shanks RA. Comput Theor Polym Sci 2001;11:57.
[28] Mckiernan RL, Sikorski P, Atkins EDT, Gido SP, Penelle J. Macromolecules 2002;35:8433.
[29] Kojio K, Fukumaru T, Furukawa M. Macromolecules 2004;37:3287.
[30] Bonart RJ. Macromol Sci Phys 1968;B2:115.
[31] Jones NA, Atkins EDT, Hill MJ, Cooper SJ, Franco L. Macromolecules 1997;30:3569.
[32] Jones NA, Atkins EDT, Hill MJ, Cooper SJ, Franco L. Macromolecules 1996;29:6011.
[33] Jones NA, Atkins EDT, Hill MJ. J Polym Sci Part B Polym Phys 2000;38:1209.
[34] Atkins EDT, Hill MJ, Jones NA, Cooper SJ. J Polym Sci Part B Polym Phys 1998;36:2401.
[35] Atkins EDT, Hill MJ, Hong SK, Keller A, Organ S. Macromolecules 1992;25:917.
[36] Atkins EDT, Hill MJ, Jones NA, Sikorski P. J Mater Sci 2000;35:5179.
[37] Sikorski P, Atkins EDT. Macromolecules 2001;34:4788.